ISSN 2176-5480

22nd International Congress of Mechanical Engineering (COBEM 2013)
November 3-7, 2013, Ribeirão Preto, SP, Brazil
Copyright © 2013 by ABCM

LINEAR AND NONLINEAR HERTIZIAN CONTACT MODELS FOR MATERIALS IN MULTIBODY DYNAMICS

Helio A. Navarro
Meire P. de Souza Braun
Department of Mechanical Engineering, São Carlos School of Engineering, University of São Paulo, Av. Trabalhador São-Carlense, 400, São Carlos, SP, 13566-590, Brazil
han@sc.usp.br, meireps@sc.usp.br

Abstract. *The Discrete Element Method is a method for simulation of a particle system. For the "soft-sphere" mechanism of particle interactions, there are several models for normal contact forces, namely Linear Spring-Dashpot, nonlinear damped Hertzian Spring-Dashpot, among others. In the present work, we compare linear and non-linear normal contact forces models for soft materials in multibody dynamics. Using the MFIX code, the models are applied in the numerical simulations of a single freely falling particle. Non-dimensional expressions, tables and graphics for linear and nonlinear models are also presented.*

Keywords: *Multibody dynamics, Contact force models, Linear and Nonlinear Spring-dashpot models, Discrete element method*

1. INTRODUCTION

Discrete Element Method (DEM) is a method based on molecular dynamics for discrete particle system. This method has been applied in several areas, e.g., in geotechnical mechanics by Cundall and Strack (1979), fluidized beds by Tsuji *et al.* (1993), segregation of granular materials by Ketterhagen *et al.* (2007), cohesive particles flows by Weber (2004), solids mixing in gas-fluidized beds by Rhodes *et al.* (2001), among other studies. A comprehensive literature review is found in the works published by Zhu *et al.* (2007), Zhu *et al.* (2008), which summarize the studies based on discrete particle simulation. In this method, the contact forces can be modeled either as "hard–sphere" or as "soft–sphere" (Crowe *et al.*, 1997). The contact forces are included in the Newton's Second Law of motion to determine the dynamic of the particles. In a hard-sphere model, the trajectories of particles are determined by momentum conserving binary collisions. In soft–sphere models, the particles are allowed to overlap slightly and the contact forces are subsequently calculated from the deformation history of the contact using a contact-force scheme. The soft–sphere method for granular dynamics simulations was developed by Cundall and Strack (1979). In the soft–sphere approach there is a mapping between the contact forces during the impact and dynamic systems. A detailed study for the impact theory is found in the book by Goldsmith (1960). The elastic mechanism in the impact modeling is first given by Hertz (1882). Timoshenko and Goodier (1970) give a classical presentation of theory of elasticity. The energy lost during impact can be associated with damping mechanisms during the contact period. Simo and Hughes (1997) present the theoretical foundations of inelasticity, its numerical formulation, and a description of computational algorithms for classical plasticity, viscoplasticity, and viscoelasticity material models.

The focus of this paper is to compare linear and nonlinear normal contact forces models for soft materials in multibody dynamics. The open source code MFIX ("Multiphase Flow with Interphase eXchanges", Syamlal *et al.* (1993)) developed at NETL ("National Energy Technology Laboratory") is used for numerical simulations. Using this code, the presented models are applied in the simulation of a single freely falling particle. Non-dimensional expressions, tables and graphics for linear and nonlinear models are also presented.

2. MATHEMATICAL MODEL

In the DEM approach, the motion of an individual particle i, with mass $m^{(i)}$ is described by Newton's laws as:

$$m^{(i)}\frac{d^2\mathbf{X}^{(i)}}{dt^2} = \mathbf{F}^{(i)}(t) = m^{(i)}\mathbf{g} + \mathbf{F}_c^{(i)}(t) \tag{1}$$

where $\mathbf{X}^{(i)}$ is the position of the mass center of the particle, $m^{(i)}\mathbf{g}$ is the gravitational force, $\mathbf{F}_c^{(i)}$ are the contact forces due the collision between particles, and $\mathbf{F}^{(i)}$ is the sum of all external forces acting on particle i. The torque of the external forces acting on the particles is calculated by:

$$\mathbf{T}^{(i)}(t) = I^{(i)}\frac{d\mathbf{w}^{(i)}(t)}{dt} \tag{2}$$

where $I^{(i)}$ is the particle mass moment of inertia given by: $I^{(i)} = \frac{2}{5}m^{(i)}{r^{(i)}}^2$, and $r^{(i)}$ is the radius of particle.

ISSN 2176-5480

The contact forces can be calculated according to the soft-sphere model proposed by Cundall and Strack (1979). This model is based on the linear spring–dashpot model which enables the analysis of some interactions between particles and between particles and wall. The soft-sphere model uses a time-step allowing that the particles remain in contact for a while. In this system, multi–particle contacts are possible. The contact forces are subsequently calculated from the level of deformation of the particles.

In the soft-sphere model, the contact forces are calculated from the overlap ("deformation"), δ, between the particles and from its relative velocity. For two particles i and j with diameters $D^{(i)}$ and $D^{(j)}$, respectively, δ_n is given by:

$$\delta_n = 0.5\left(D^{(i)} + D^{(j)}\right) - \left|\mathbf{X}^{(i)} - \mathbf{X}^{(j)}\right| \tag{3}$$

where $\mathbf{X}^{(i)}$ and $\mathbf{X}^{(j)}$ are the positions of the mass center of the particles i and j, respectively. For these particles with linear and angular velocities equal $\mathbf{V}^{(i)}$ and $\mathbf{w}^{(i)}$, and $\mathbf{V}^{(j)}$ and $\mathbf{w}^{(j)}$, respectively, the relative velocity of the point of contact is:

$$\mathbf{V}_{ij} = \mathbf{V}^{(j)} - \mathbf{V}^{(i)} + \mathbf{w}^{(j)} \times \mathbf{R}^{(j)} - \mathbf{w}^{(i)} \times \mathbf{R}^{(i)} \tag{4}$$

where $\mathbf{R}^{(i)}$ and $\mathbf{R}^{(j)}$ are vectors from the mass center of the particles i and j, respectively, to the contact point (see Fig. 1).

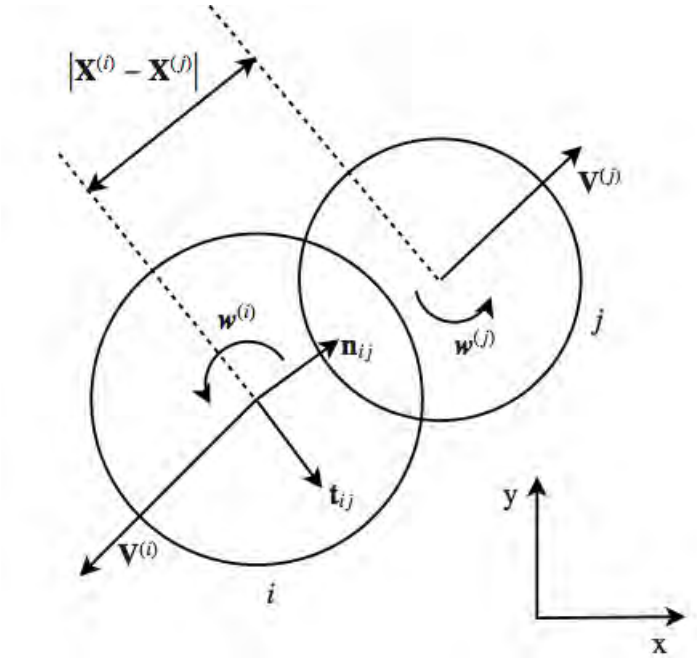

Figure 1. Schematic of two particles in contact (soft-sphere model).

The normal $\mathbf{V}_{n,ij}$ and the tangential components $\mathbf{V}_{t,ij}$ of relative contact velocity are given by:

$$\mathbf{V}_{n,ij} = (\mathbf{V}_{ij}.\mathbf{n}_{ij})\mathbf{n}_{ij} \tag{5}$$

$$\mathbf{V}_{t,ij} = \mathbf{V}_{ij} - \mathbf{V}_{n,ij} \tag{6}$$

$\mathbf{n}_{ij} = (\mathbf{X}^{(j)} - \mathbf{X}^{(i)})/|\mathbf{X}^{(j)} - \mathbf{X}^{(i)}|$ is the normal unit vector along the contact line pointing from particle i to particle j. In the soft-sphere model, the overlap (δ) between two particles is represented by a spring-dashpot system.

The contact force ($\mathbf{F}_c^{(i)}$) acting on a particle i, at time t, is calculated as the sum of the contact force of all particles j that are in contact with the particle i:

$$\mathbf{F}_c^{(i)}(t) = \sum_{j=1\ j\neq i}^{N} (\mathbf{F}_{n,ij}(t) + \mathbf{F}_{t,ij}(t)) \tag{7}$$

where $\mathbf{F}_{n,ij}$ and $\mathbf{F}_{t,ij}$ are the normal and tangential components of the contact force between the particles i and j.

The total torque acting on the particle i is calculated by:

$$\mathbf{T}^{(i)}(t) = \sum_{j=1\ j\neq i}^{N} \left(\mathbf{R}^{(i)} \times \mathbf{F}_{t,ij}(t)\right) \tag{8}$$

ISSN 2176-5480

From the Eq. (7), the normal and tangential components of the contact force, $\mathbf{F}_c^{(i)}$, are decomposed into spring conservative force ($\mathbf{F}^S$) and dashpot dissipative force ($\mathbf{F}^D$):

$$\mathbf{F}_{n,ij}(t) = \mathbf{F}^S_{n,ij} + \mathbf{F}^D_{n,ij} \tag{9}$$

$$\mathbf{F}_{t,ij}(t) = \mathbf{F}^S_{t,ij} + \mathbf{F}^D_{t,ij} \tag{10}$$

2.1 Contact force: linear model

In the soft-sphere model, the overlap (δ) between two particles is represented by a linear spring-dashpot system. The Hooke's law ($F(\delta_n) = k\delta_n$) is used for describing the elastic force. The spring stiffness and the dashpot damping coefficients in the normal direction are k_n and η_n, respectively, and the spring stiffness and the dashpot damping coefficients in the tangential direction are k_t and η_t, respectively.

The normal and tangential spring forces, ($\mathbf{F}^S_{n,ij}$) and ($\mathbf{F}^S_{t,ij}$), respectively, are calculated based on the overlap between the collision of particles:

$$\mathbf{F}^S_{n,ij} = -k_n \delta_n \mathbf{n}_{ij} \tag{11}$$

$$\mathbf{F}^S_{t,ij} = -k_t \delta_{\mathbf{t}} \tag{12}$$

where k_n is normal stiffness spring coefficient, k_t is tangential stiffness spring coefficient, δ_n is the normal overlap between particles i and j and $\delta_{\mathbf{t}}$ is the vector of the tangential displacement between particles i and j (see e.g. Garg *et al.* (2012)).

For the case of Coulomb friction between the particles, if the condition bellow is satisfied during any contact time,

$$|\mathbf{F}_{t,ij}| > \mu \, |\mathbf{F}_{n,ij}| \tag{13}$$

then the sliding occurs and the tangential contact force is calculated as:

$$\mathbf{F}_{t,ij} = -\mu \, |\mathbf{F}_{n,ij}| \, \mathbf{t}_{ij} \tag{14}$$

where μ is the friction coefficient and $\mathbf{t}_{ij} = \mathbf{V}_{t,ij}/|\mathbf{V}_{t,ij}|$ is the tangential unit vector.

The normal and tangential dashpot forces, ($\mathbf{F}^D_{n,ij}$) and ($\mathbf{F}^D_{t,ij}$), respectively, are calculated based on normal and tangential components of relative contact velocity:

$$\mathbf{F}^D_{n,ij} = -\eta_n \mathbf{V}_{n,ij} \tag{15}$$

$$\mathbf{F}^D_{t,ij} = -\eta_t \mathbf{V}_{t,ij} \tag{16}$$

where η_n and η_t are normal and tangential damping coefficients, respectively.

The normal stiffness spring k_n and the normal damping coefficient η_n for collision between particles i and j belong the solid-phases m and l are calculated applying the Newton's Second Law in the normal direction by the acting normal contact forces Eq.(9). This LSD model, with initial conditions $\delta_n(0) = 0$ and $\mathbf{V}_{n,ij}(0) = \mathbf{V}_0$, has analytic solution for the normal overlap that allows to determine the normal restitution coefficient, e_n and the collision duration, $t = t_{c,n}$. Therefore, considering $\delta_n = 0$ at $t = t_{c,n}$ and $\mathbf{V}_{n,ij}(t_{c,n}) = -e_n \mathbf{V}_0$, the quantities e_n and $t_{c,n}$ are given by (see e.g. Shäfer *et al.* (1996)):

$$e_n = \exp\left(-\frac{\eta_n}{2m_{eff}} t_{c,n}\right) \tag{17}$$

$$t_{c,n} = \pi \left(\frac{k_n}{m_{eff}} - \frac{\eta_n^2}{4m_{eff}^2}\right)^{-1/2} \tag{18}$$

where $1/m_{eff} = 1/m_m + 1/m_l$ is the effective mass. From Eq. (17) and Eq. (18), k_n and η_n are expressed as:

$$k_n = \frac{m_{eff}}{t_{c,n}^2}(\ln^2 e_n + \pi^2) \tag{19}$$

$$\eta_n = -2\sqrt{m_{eff} k_n} \frac{\ln e_n}{\sqrt{\ln^2 e_n + \pi^2}} \tag{20}$$

If the values of e_n and $t_{c,n}$ are known by experimental measures, the quantities k_n and η_n can be determined by Eq. (19) and Eq. (20), respectively. Usually, in numerical simulations, we only have the value for e_n, so we need a procedure

ISSN 2176-5480

for estimate the value for k_n in the LSD model. Sun *et al.* (2007) state that the value of the spring constant should be large enough to avoid particle interpenetration, yet not so large as to require an unreasonably small simulation time–step.

Following the work of Shäfer *et al.* (1996), the tangential spring stiffness coefficient can be assumed to be equal to two-sevenths of the normal stiffness coefficient (i.e., $k_t = 2/7k_n$). The tangential damping coefficient can be taken to be half of normal damping coefficient,i.e. η_t=0.5η_n (Silbert *et al.* (2001), Silbert *et al.* (2003)).

Now, we detail the motion of the particle in the normal direction. The equation of motion for the overlap in the normal direction, δ_n, describing the collisions of two particles can be written as:

$$m_{eff}\ddot{\delta}_n = -k_n\delta_n - \eta_n\dot{\delta}_n \tag{21}$$

or

$$\ddot{\delta}_n + 2\Psi\dot{\delta}_n + \Omega_0^2\delta_n = 0 \tag{22}$$

where $\Omega_0 = \sqrt{k_n/m_{eff}}$ is the frequency of the undamped harmonic oscillator and $\Psi = \eta_n/(2m_{eff})$ is the damping coefficient responsible for energy dissipation.

The solution for the differential equation of the damped harmonic oscillator, Eqs. 21,22, for the under-damped case ($\Omega_0 > \Psi$), with initial conditions $\delta_n(0) = 0$ and $\dot{\delta}_n(0) = v_0$ is

$$\delta_n(t) = (v_0/\Omega)\exp(-\Psi t)\sin(\Omega t) \tag{23}$$

$$\dot{\delta}_n(t) = (v_0/\Omega)\exp(-\Psi t)(-\Psi\sin(\Omega t) + \Omega\cos(\Omega t)) \tag{24}$$

where v_0 is the initial relative velocity and $\Omega = \sqrt{\Omega_0^2 - \Psi^2}$ is the frequency of the damped oscillator. The LSD model is widely used due to the existence of simple analytic solution for the overlap and relationships between the parameters k_n and η_n. The duration of a contact can be determined from $\delta_n(t_{c,n}) = 0$ in Eq. 23 which gives $t_{c,n} = \pi/\Omega$ (or Eq. 18), so that the relative velocity just after contact equals $\dot{\delta}_n(t_{c,n}) = -v_0\exp(-\Psi t_{c,n})$. The normal coefficient of restitution is given by Eq. 17 or

$$e_n = -\frac{\dot{\delta}_n(t_{c,n})}{\dot{\delta}_n(0)} = \exp(-\pi\Psi/\Omega) \tag{25}$$

The inverse relationship of 25 allows to compute the value for the parameter Ψ or η_n, see Eq. 20, if the experimental value for e_n is known,

$$\Psi = \frac{-\ln e_n}{\sqrt{\ln^2 e_n + \pi^2}}\Omega_0 \tag{26}$$

The linear model predicts that the normal coefficient of restitution e_n and contact duration $t_{c,n}$ are independent of impact velocity v_0 (see Eqs. 25 and 18). The maximum overlap can also be derived from $\dot{\delta}_n(t_{max}) = 0$, Eqs. 23 and 24, and it is expressed by

$$\delta_{max} = (v_0/\Omega_0)\exp(-\frac{\arctan(\beta)}{\beta}) \tag{27}$$

where $\beta = -\Omega/\Psi = \pi/\ln e_n$ for $e_n < 1.0$. The contact duration can be re-written as

$$t_{c,n} = \frac{\pi}{\Omega_0}\sqrt{(1 + \frac{1}{\beta^2})} \tag{28}$$

For the perfectly elastic collision ($e_n = 1.0$), $\Psi = \eta_n = 0$, and we have the following expressions for the maximum overlap and the contact duration: $\delta_{max} = v_0/\Omega_0$ and $t_{c,n} = \pi/\Omega_0$.

Using the following dimensionless parameters in Eq.22:

$$\delta_n^* = \frac{\delta_n}{v_0}\Omega_0, \quad \delta_n^{*\prime} = \frac{\dot{\delta}_n}{v_0}, \quad t^* = t\Omega_0$$

The equation of motion for the dimensionless overlap in the normal direction, δ_n^*, can be written as:

$$\delta_n^{*\prime\prime} + 2\nu^*\delta_n^{*\prime} + \delta_n^* = 0 \tag{29}$$

where the primes denote derivatives with respect to t^*. The parameter ν^* is the dimensionless damping coefficient given by ($0 < e_n \leq 1$)

$$\nu^* = \frac{\Psi}{\Omega_0} = \frac{-\ln e_n}{\sqrt{\ln^2 e_n + \pi^2}} \tag{30}$$

ISSN 2176-5480

where $0 \leq \nu^* < 1$. The solution for the dimensionless overlap equation (Eq. 29) for the under-damped case ($0 \leq \nu^* < 1$) with initial conditions $\delta_n^*(0) = 0$ and $\delta_n^{*\prime}(0) = 1$ is given by

$$\delta_n^*(t^*) = (1/\Omega^*)\exp(-\nu^* t^*)\sin(\Omega^* t^*) \tag{31}$$

where $\Omega^* = \sqrt{1-\nu^{*2}}$ is the dimensionless frequency of the damped oscillator.

The dimensionless maximum overlap and the dimensionless contact duration are given by:

$$\delta_{max}^* = \exp(-\frac{\arctan(\beta^*)}{\beta^*}) \tag{32}$$

$$t_{c,n}^* = \pi\sqrt{(1+\frac{1}{\beta^{*2}})} \tag{33}$$

where $\beta^* = -\Omega^*/\nu^* = \pi/\ln e_n = \beta$, for $0 < e_n < 1.0$. For the perfectly elastic collision ($e_n = 1.0$), the dimensionless damping coefficient is equal to zero ($\nu^* = 0$). In this case, the dimensionless maximum overlap and the dimensionless contact duration are expressed by $\delta_{max}^* = 1.0$ and $t_{c,n}^* = \pi$, respectively.

Fig. 2 illustrates curves for dimensionless overlap, δ^*, versus dimensionless time for viscous damping contact representing several values of the normal restitution coefficient ($e_n = 0.9, 0.7, 0.5, 0.3, 0.1$). Theses graphs are obtained until the contact duration. In this figure the contact duration increases as e_n decreases (see Table 1). Larger contact duration is desirable since larger simulation integration time steps may be used. We can also see that contact duration is independent of impact velocity, opposite of real collisions (see Goldsmith (1960), Lun and Savage (1986)). The maximum overlap also increases as e_n increases (see Table 1). The larger values for overlaps make the soft-model base on the geometrically rigid particle assumption (limited to small deformations or overlaps) less accurate and can cause physical modeling errors due to excluded volume effects.

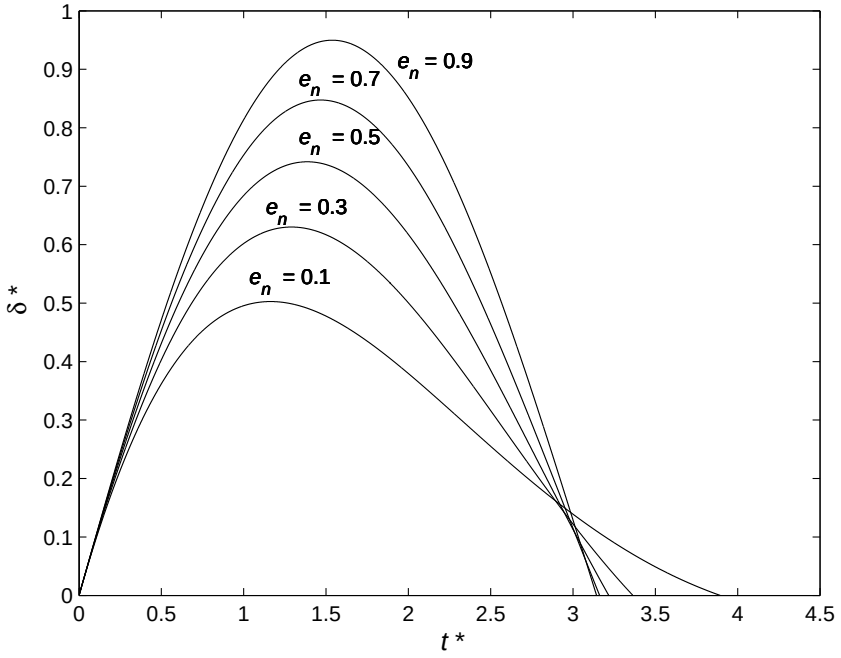

Figure 2. Dimensionless overlap (linear model).

Table 1 shows, for several values of the normal restitution coefficient ($e_n = 1.0, 0.9, 0.7, 0.5, 0.3, 0.1$), the following dimensionless parameters: damping coefficient ν^*, time at maximum overlap t_{max}^*, maximum overlap δ_{max}^*, contact duration $t_{c,n}^*$, acceleration at initial time $a^*(0)$, and acceleration at the end of contact $a^*(t_{c,n}^*)$, respectively.

2.2 Contact force: nonlinear model

The collisions between particle-particle and particle wall can also be described with Hertzian contact theory, Hertz (1882), Goldsmith (1960). The collision of two elastic spheres is described by the integration of Hooke's Law over the

ISSN 2176-5480

Table 1. Dimensionless parameters for the linear model.

e_n	ν^*	t^*_{max}	δ^*_{max}	$t^*_{c,n}$	$a^*(0)$	$a^*(t^*_{c,n})$
1	0	1.5708	1	3.1416	0	0
0.9	0.0335	1.5381	0.9498	3.1434	-0.0670	0.0603
0.7	0.1128	1.4671	0.8475	3.1618	-0.2256	0.1579
0.5	0.2155	1.3862	0.7418	3.2172	-0.4309	0.2155
0.3	0.3579	1.2903	0.6302	3.3644	-0.7157	0.2147
0.1	0.5912	1.1635	0.5027	3.8951	-1.1823	0.1182

deformation area that results in a nonlinear relationship known as Hertz's Law ($F(\delta_n) = k_{n,Hz}\delta_n^{3/2}$) Hertz (1882), where $k_{n,Hz}$ is described below. So, the normal and tangential spring forces, ($\mathbf{F}^S_{n,ij}$) and ($\mathbf{F}^S_{t,ij}$), are given by:

$$\mathbf{F}^S_{n,ij} = -k_{n,Hz}\delta_n^{\frac{1}{2}}\delta_n\mathbf{n}_{ij} \tag{34}$$

$$\mathbf{F}^S_{t,ij} = -k_{t,Hz}\delta_n^{\frac{1}{2}}\delta_{\mathbf{t}} \tag{35}$$

Hunt and Grossley (1975) derived a expression for the damping term $\lambda\delta_n(t)^p\dot{\delta_n}(t)^q$. Here, we assume $q = 1$, but as discussed by Hunt and Grossley (1975) other choices are suitable for the index q. Considering $p = 1/4$, an expression for dissipative force proposed by Tsuji *et al.* (1992) represents the normal and tangential dashpot forces, ($\mathbf{F}^D_{n,ij}$) and ($\mathbf{F}^D_{t,ij}$), that are described by:

$$\mathbf{F}^D_{n,ij} = -\eta_{n,Hz}{\delta_n}^{1/4}\mathbf{V}_{n,ij} \tag{36}$$

$$\mathbf{F}^D_{t,ij} = -\eta_{t,Hz}{\delta_n}^{1/4}\mathbf{V}_{t,ij} \tag{37}$$

the nonlinear normal and tangential spring stiffnesses between contacting particle i and j, $k_{n,Hz}$, $k_{t,Hz}$, are calculated as:

$$k_{n,Hz} = \frac{4}{3}E_{eff}\sqrt{r_{eff}} \tag{38}$$

$$k_{t,Hz} = \frac{16}{3}G_{eff}\sqrt{r_{eff}} \tag{39}$$

and the nonlinear normal and tangential damping coefficients, $\eta_{n,Hz}$, $\eta_{t,Hz}$ are related to the nonlinear spring stiffness and restitution coefficient as:

$$\eta_{n,Hz} = -\sqrt{5}\sqrt{m_{eff}k_{n,Hz}}\frac{\ln e_n}{\sqrt{\ln^2 e_n + \pi^2}} \tag{40}$$

$$\eta_{n,Hz} = -\sqrt{5}\sqrt{m_{eff}k_{t,Hz}}\frac{\ln e_t}{\sqrt{\ln^2 e_t + \pi^2}} \tag{41}$$

where E_{eff} and G_{eff} are the effective Young's modulus and effective shear modulus expressed by $1/E_{eff} = (1 - \sigma_m^2)/E_m + (1 - \sigma_l^2)/E_l$ and $1/G_{eff} = (2 - \sigma_m)/G_m + (2 - \sigma_l)/G_l$, respectively, and E_m and E_l are the Young's moduli, and σ_m and σ_l are the Poisson ratios for m^{th} and l^{th} solid-phases, respectively. G_m and G_l are the shear moduli for m^{th} and l^{th} solid-phases calculated as $G_m = E_m/2(1 + \sigma_m)$, $G_l = E_l/2(1 + \sigma_l)$, and r_{eff} is the effective radius expressed by $1/r_{eff} = 1/r_m + 1/r_l$, where r_m and r_l are the radii of the particles.

The equation of motion for the normal overlap is expressed by the nonlinear damped Hertzian oscillator equation:

$$m_{eff}\ddot{\delta}_n = -k_{n,Hz}\delta_n^{3/2} - \eta_{n,A}{\delta_n}^{1/4}\dot{\delta_n} \tag{42}$$

Using the following dimensionless parameters in Eq.42:

$$\delta^*_n = \delta_n(\frac{k_{n,Hz}}{v_0^2 m_{eff}})^{2/5}, \quad \delta^{*\prime}_n = \frac{\dot{\delta}_n}{v_0}, \quad t^* = t(\frac{k_{n,Hz}v_0^{1/2}}{m_{eff}})^{2/5}$$

where v_0 is the impact velocity. The equation of motion for the dimensionless overlap in the normal direction, δ^*_n, can be written as:

$$\delta^{*\prime\prime}_n + 2\nu^*_A\delta^{*1/4}_n\delta^{*\prime}_n + \delta^{*3/2}_n = 0 \tag{43}$$

ISSN 2176-5480

where the primes denote derivatives with respect to t^*. The parameter ν_A^* is the dimensionless damping coefficient given by

$$\nu_A^* = \frac{\eta_{n,Hz}}{2\sqrt{(m_{eff}k_{n,Hz})}} \tag{44}$$

The equation 43 can be solved numerically with initial conditions $\delta_n^*(0) = 0$ and $\delta_n^{*\prime}(0) = 1$ for determining a set of dimensionless overlaps $\delta_{n,i}^*$ for instants t_i^*.

Fig. 3 shows graphs for the nonlinear model for dimensionless overlap versus dimensionless time for several values of the Hertzian dimensionless damping coefficient ($\nu_A^* = 0, 0.1, 0.25, 0.4, 0.6$). As before, theses graphs are plotted until the contact duration $t_{c,n}^*$. In Fig. 3 the contact duration increases as ν_A^* increases. We can also see that contact duration is independent of impact velocity and that the maximum overlap also increases as ν_A^* decreases.

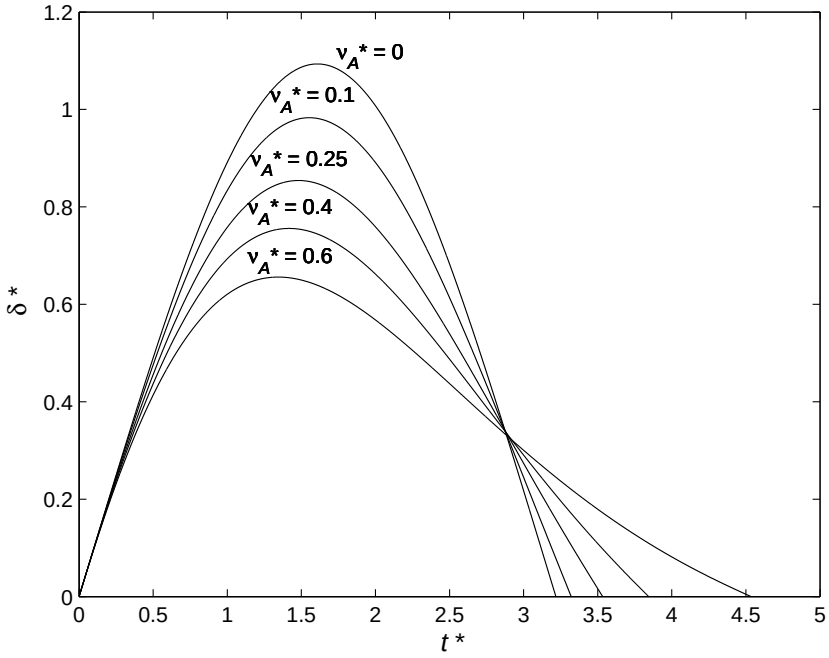

Figure 3. Dimensionless overlap (nonlinear model).

Table 2 shows, for several values of the damping coefficient, (ν_A^*), the following dimensionless parameters: normal restitution coefficient e_n, time at maximum overlap t_{max}^*, maximum overlap δ_{max}^*, contact duration $t_{c,n}^*$, acceleration at initial time $a^*(0)$, and acceleration at end of contact $a^*(t_{c,n}^*)$, respectively. These parameters can be computed based on dimensionless overlap time solution. The normal coefficient of restitution is computed by $e_n = -\delta_n^{*\prime}(t_{c,n}^*)$ and acceleration by $a^* = v^{*\prime}$.

Table 2. Dimensionless parameters for the nonlinear model.

ν_A^*	e_n	t_{max}^*	δ_{max}^*	$t_{c,n}^*$	$a^*(0)$	$a^*(t_{c,n}^*)$
0	1.0000	1.6090	1.0936	3.2181	0	0
0.02	0.9453	1.5976	1.0693	3.2366	-0.0018	0.0034
0.04	0.8936	1.5864	1.0465	3.2562	-0.0036	0.0050
0.1	0.7542	1.5542	0.9830	3.3213	-0.0089	0.0089
0.4	0.3001	1.4181	0.7557	3.8449	-0.0358	0.0096
0.6	0.1356	1.3449	0.6559	4.5368	-0.0536	0.0057

3. RESULTS

In this section we describe numerical simulation of a single freely falling particle. We compute the contact forces using two models: linear and nonlinear. In the analyzed problem, a single smooth frictionless spherical particle is dropped from a specified height. The particle freely falls under gravity and bounces upon collision with a fixed wall. Figure 4 shows a

ISSN 2176-5480

model of a ball falling on a stationary surface. This classical bouncing ball problem has been applied by several authors (e.g. Chen *et al.* (2007), Flores *et al.* (2011), Garg *et al.* (2012), Jankowski (2005), Ye *et al.* (2009)). Following the work of Garg *et al.* (2012) and Chen *et al.* (2007), we have studied a single $0.2\,\text{m}$ particle diameter falling and bouncing in a wall.

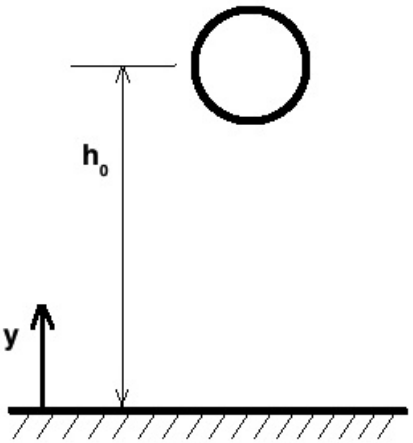

Figure 4. Schematic for the free fall of a single particle.

3.1 Linear model

In this section we use the linear model for determination of the contact forces. The particle parameters are taken from Chen *et al.* (2007) and reproduced in Table 3. The impact velocity of the particle with the wall is $v_0 = -\sqrt{2g(h_0 - r_p)} = -2.801\,\text{m/s}$, where r_p is the particle radius.

Table 3. Simulation parameters for single freely falling particle: linear case.

Fall height	$0.5\,\text{m}$
Particle diameter	$0.2\,\text{m}$
Particle density	$2600\,\text{kg/m}^3$
Normal particle–wall restitution coefficients	0.9 and 0.7
Particle–wall normal spring stiffness coefficients	$k_n = 7.94 \times 10^4\,\text{N/m}$ and $k_n = 7.77 \times 10^4\,\text{N/m}$
Particle–wall tangential spring stiffness coefficient	$k_t = k_n$
Particle–wall tangential damping coefficient	$\eta_t = \eta_n$
Acceleration of gravity	$9.81\,\text{m/s}^2$

Now we illustrate the position and velocity time-history. The MFIX–DEM code has been used in the simulations. A similar test for free falling particle was verified in the work developed by Garg *et al.* (2012). First we simulate a single freely falling particle with a normal restitution coefficient equal to 0.9. The normal spring stiffness coefficient used is $k_n = 7.94 \times 10^4\,\text{N/m}$ (Navarro and Souza-Braun (2013)). Figure 5 shows the particle center position y and the particle velocity v versus time (from $t = 0\,\text{s}$ to $t = 1.6\,\text{s}$). The contact is modeled with linear model and the particle rebounds after each impact with the wall. We can see the energy lost due to dissipative contact force. The duration of contact occurs for values of the particle center position $y < 0.1\,\text{m}$, where the repulsive force acts. During the total simulation time $t = 1.6\,\text{s}$, the particle collided with the wall three times.

Now, we describe simulations using the normal restitution coefficient equal to 0.7. The normal spring stiffness coefficient used is $k_n = 7.77 \times 10^4\,\text{N/m}$ (Navarro and Souza-Braun (2013)). Figure 6 shows the results of the particle kinematics (center position y and the particle velocity v versus time), when the normal coefficient of restitution is $e_n = 0.7$. Similarly to the case analyzed before, when the particle hits the wall, a contact occurs and the particle is rebounded. As the coefficient of restitution is smaller than a unit, the particle jumps less high after each contact. The contact duration in each particle bounce is smaller and decreases until zero when the particle remains on the ground. In Fig. 6, we can see seven collisions of the particle with the wall.

ISSN 2176-5480

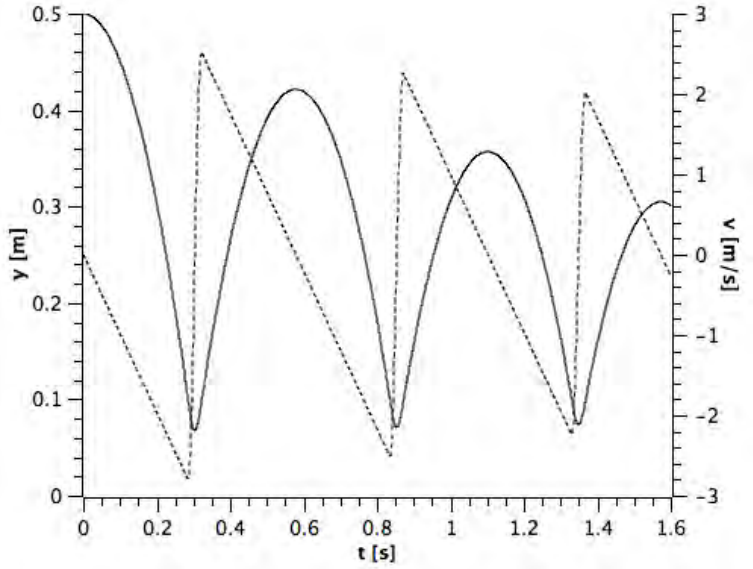

Figure 5. Particle kinematics ($k_n = 7.94 \times 10^4$ N/m and $e_n = 0.9$, linear model): particle center position y (solid line); particle velocity (dashed line).

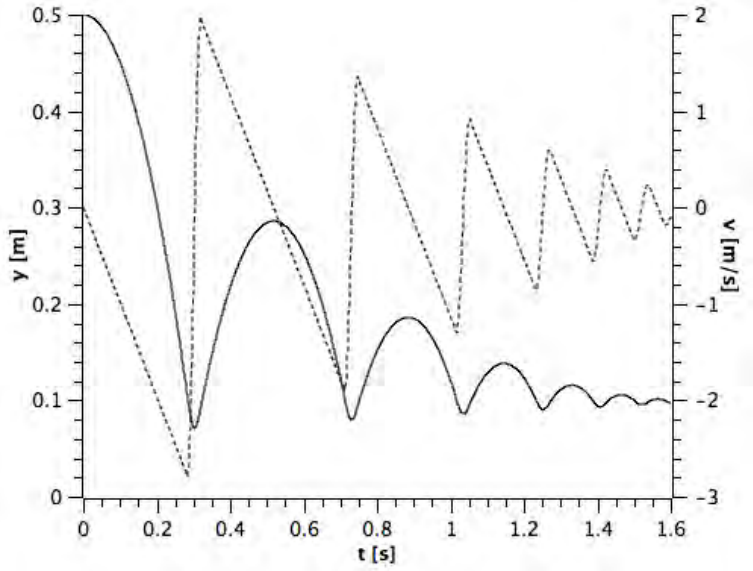

Figure 6. Particle kinematics ($k_n = 7.77 \times 10^4$ N/m and $e_n = 0.7$, linear model): particle center position y (solid line); particle velocity (dashed line).

3.2 Nonlinear model

As the linear model, the simulations parameters are also taken (Chen *et al.*, 2007) (see Table 4) and the impact velocity of the particle with the wall is $v_0 = -2.801$ m/s. We applied for computation of the contact forces a nonlinear model based on Eqs. 34, 35, 36, and 37.

Figure 7 also shows the particle center position y and the particle velocity v versus time (from $t = 0$ s to $t = 1.6$ s). The contact force is modeled with nonlinear model and the particle rebounds after each impact with the wall. This figure is similar with Fig. 5. As the normal restitution coefficient is close to unity, the damping effect is small and the nonlinear elasticity does not influence the position and velocity curves.

Now, we describe simulations using the normal restitution coefficient equal to 0.7. Figure 8 shows the results of the particle kinematics. Similarly to the case analyzed before, when the particle hits the wall, a contact occurs and the particle is rebounded. As the coefficient of restitution is smaller than a unit, the particle jumps less high after each contact. The contact duration in each particle bounce is smaller and decreases until zero when the particle remains on the ground. In Fig. 8, we can see five collisions of the particle with the wall. The number of collision is smaller in the nonlinear case because of effect of viscous damping and nonlinear elasticity.

ISSN 2176-5480

Table 4. Simulation parameters for single freely falling particle: nonlinear case.

Fall height	0.5 m
Particle diameter	0.2 m
Particle density	2600 kg/m^3
Particle Young's modulus	1.6916 MPa
Wall Young's modulus	5.0748 MPa
Normal particle–wall restitution coefficients	0.9 and 0.7
Tangential particle–wall restitution coefficient	1.0
Particle and wall Poisson's ratios	0
Acceleration of gravity	9.81 m/s^2

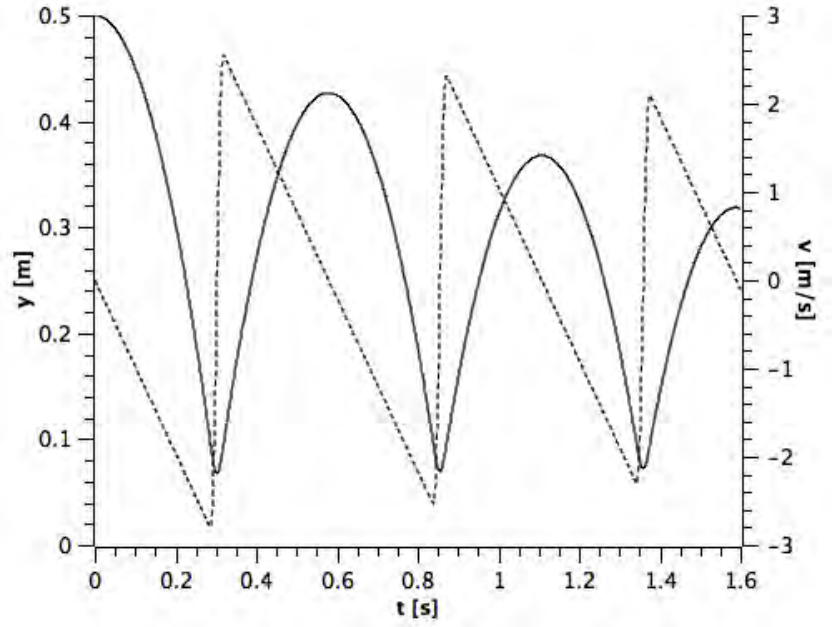

Figure 7. Particle kinematics ($e_n = 0.9$, nonlinear model): particle center position y (solid line); particle velocity (dashed line).

4. CONCLUSIONS

This paper presents the DEM method with "soft-sphere" mechanism for simulation of a particle system. The contact forces are computed by linear and nonlinear models based on mass-spring-damper system. We derive the fundamental equations for these two models. Using the MFIX code, the models are applied in the numerical simulations of a single freely falling particle. Both models give similar results for the particle kinematics time-history. Non-dimensional expressions, tables and graphics for linear and nonlinear models are also presented.

5. ACKNOWLEDGEMENTS

The authors acknowledge the financial supports received from *Fundação de Amparo e Pesquisa do Estado de São Paulo* (FAPESP - Proc.2010/19769-4 and Proc.2012/03468-0), *Coordenação de Aperfeicoamento de Pessoal de Nível Superior* (CAPES) and also the *Conselho Nacional de Desenvolvimento Científico e Tecnológico* (CNPq). The authors fully appreciate the support received from NETL (National Energy Technology Laboratory) that develops MFIX code, `https://www.mfix.org`.

6. REFERENCES

Chen, F., Drumm, E.C. and Guiochon, G., 2007. "Prediction/verification of particle motion in one dimension with the discrete–element method". *International Journal of Geomechanics*, Vol. 7, pp. 344–352.

Crowe, C., Sommerfeld, M. and Tsuji, Y., 1997. *Multiphase Flows with Droplets and Particles*. CRC Press, Boca Raton.

Cundall, P.A. and Strack, O.D.L., 1979. "A discrete numerical model for granular assemblies". *Géotechnique*, Vol. 29, No. 1, pp. 47–65.

ISSN 2176-5480

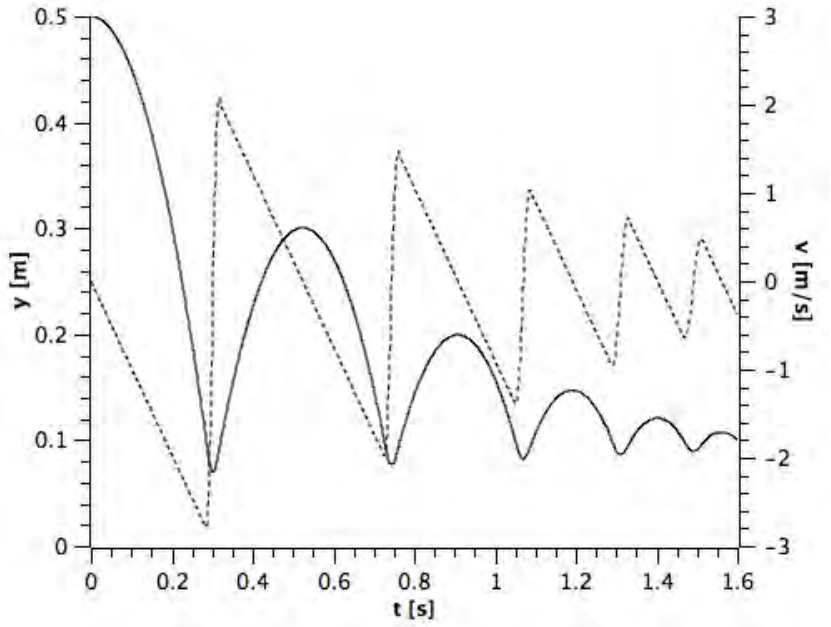

Figure 8. Particle kinematics ($e_n = 0.7$, nonlinear model): particle center position y (solid line); particle velocity (dashed line).

Flores, P., Machado, M., Silva, M.T. and Martins, J.M., 2011. "On the continuous contact force models for soft materials in multibody dynamics". *Multibody System Dynamics*, Vol. 25, pp. 357–375.

Garg, R., Galvin, J., Li, T. and Pannala, S., 2012. "Open-source MFIX–DEM software for gas–solids flows: Part I–Verification studies". *Powder Technology*, Vol. 220, pp. 122 – 137.

Goldsmith, W., 1960. *Impact*. Edward Arnold Publishers Ltd., London.

Hertz, H., 1882. "Über die Berührung fester elastischer Körper". *Journal für die Reine und Angewandte Mathematik*, Vol. 92, pp. 156 – 171.

Hunt, K.H. and Grossley, F.R.E., 1975. "Coefficient of restitution interpreted as damping in vibroimpact". *ASME Journal of Applied Mechanics*, Vol. 7, pp. 440 – 445.

Jankowski, R., 2005. "Non–linear viscoelastic modelling of earthquake-induced structural pounding". *Earthquake Engineering and Structural Dynamics*, Vol. 34, No. 6, pp. 595–611.

Ketterhagen, W.R., Curtis, J.S., Wassgren, C.R., Kong, A., Narayan, P.J. and Hancock, B.C., 2007. "Granular segregation in discharging cylindrical hoppers: A discrete element and experimental study". *Chemical Engineering Science*, Vol. 62, No. 22, pp. 6423 – 6439.

Lun, C.K.K. and Savage, S.B., 1986. "The effects on an impact velocity dependent coefficient of restitution on stresses developed by sheared granular materials". *Acta Mechanica*, Vol. 63, No. 1, pp. 15–44.

Navarro, H.A. and Souza-Braun, M.P., 2013. "Determination of the normal spring stiffness coefficient in the linear spring–dashpot contact model of discrete element method". *Powder Technology*, Vol. 246, pp. 707 – 722.

Rhodes, M.J., Wang, X.S., Nguyen, M., Stewart, P. and Liffman, K., 2001. "Study of mixing in gas-fluidized beds using a DEM model". *Chemical Engineering Science*, Vol. 56, No. 8, pp. 2859 – 2866.

Shäfer, J., Dippel, S. and Wolf, D.E., 1996. "Force schemes in simulations of granular materials". *Journal de Physique I France*, Vol. 6, No. 1, pp. 5–20.

Silbert, L.E., Ertas, D., Grest, G.S., Halsey, T.C., Levine, D. and Plimpton, S.J., 2001. "Granular flow down an inclined plane: Bagnold scaling and rheology". *Physical Review E*, Vol. 64, p. 051302.

Silbert, L.E., Landry, J.W. and Grest, G.S., 2003. "Granular flow down a rough inclined plane: transition between thin and thick piles". *Physics of Fluids*, Vol. 15, pp. 1–10.

Simo, J.C. and Hughes, T.J.R., 1997. *Computational Inelasticity*. Springer–Verlag, New York.

Sun, J., Battaglia, F. and Subramaniam, S., 2007. "Hybrid two-fluid DEM simulation of gas–solid fluidized beds". *Journal of Fluids Engineering*, Vol. 129, No. 11, pp. 1394–1403.

Syamlal, M., Rogers, W. and O'Brien, T.J., 1993. "MFIX documentation theory guide". Technical Report DOE/METC-94/1004, National Energy Technology Laboratory, US Department of Energy. URL `https://mfix.netl.doe.gov/documentation/Theory.pdf`.

Timoshenko, S.P. and Goodier, J.N., 1970. *Theory of Elasticity*. McGraw–Hill, New York.

Tsuji, Y., Kawaguchi, T. and Tanaka, T., 1993. "Discrete particle simulation of two-dimensional fluidized bed". *Powder Technology*, Vol. 77, No. 1, pp. 79 – 87.

ISSN 2176-5480

Tsuji, Y., Tanaka, T. and Ishida, T., 1992. "Lagrangian numerical simulation of plug flow of cohesionless particles in a horizontal pipe". *Powder Technology*, Vol. 71, No. 3, pp. 239 – 250.

Weber, M.W., 2004. *Simulation of cohesive particle flows in granular and gas–solid systems*. PhD Thesis, University of Colorado, Boulder, Colorado, USA.

Ye, K., Li, L. and Zhu, H., 2009. "A note on the Hertz contact model with nonlinear damping for pounding simulation". *Earthquake Engineering and Structural Dynamics*, Vol. 38, No. 9, pp. 1135–1142.

Zhu, H.P., Zhou, Z.Y., Yang, R.Y. and Yu, A.B., 2007. "Discrete particle simulation of particulate systems: Theoretical developments". *Chemical Engineering Science*, Vol. 62, No. 13, pp. 3378 – 3396.

Zhu, H.P., Zhou, Z.Y., Yang, R.Y. and Yu, A.B., 2008. "Discrete particle simulation of particulate systems: A review of major applications and findings". *Chemical Engineering Science*, Vol. 63, No. 23, pp. 5728 – 5770.

7. RESPONSIBILITY NOTICE

The authors are the only responsible for the printed material included in this paper.